Magnetic Susceptibility of $Al_2O_3:Ti^{3+}$ †

Alfred R. Smith, Donald J. Arnold, and Raymond W. Mires
Department of Physics, Texas Technological College, Lubbock, Texas 79409
(Received 13 May 1970)

Results of a temperature-dependent study of the magnetic susceptibility and anisotropy for $Al_2O_3:Ti^{3+}$ are reported for the first time. Measurements were made using a Faraday balance and a sensitive torsion balance over the temperature range 1–350 °K. The data could be described using the previously observed spectroscopic parameters, and estimates of the Van Vleck susceptibility for all three trigonal states are obtained. The value $g_{\perp}^2 - g_{\parallel}^2 = -0.40$ for the second excited state differs in sign from Macfarlane's calculated value.

I. INTRODUCTION

The Al_2O_3 crystal has been used as a host for the study of practically all the transition-metal ions. Some of these ions have been intentionally substituted for the Al^{3+} ion, while others seem to be a naturally occurring impurity. The transition-metal ion Ti^{3+} has a single $3d$ electron in the octahedral environment of the corundum lattice, and for this reason one might expect that it would have been the first such impurity to receive any attention. However, only very recently has much effort been made to understand the $Al_2O_3:Ti^{3+}$ system. This was probably due to two reasons: (a) Good single crystals for experimental work have been extremely hard to obtain and (b) the operation of a dynamic Jahn-Teller effect[1–3] hampered the development of the necessary theory. The first really significant experimental results were reported by McClure[4] on the optical spectra followed by the far-infrared spectra by Nelson *et al.*[5] This last work was the first to report experimental energy spacings within the two trigonal manifolds when the free ion is incorporated into the corundum structure. A very short time later, Macfarlane *et al.*[6] made a second-order dynamic Jahn-Teller calculation using some "typical" values for several crystal field parameters to explain the energy spacings as well as calculate the g factors for the spin-orbit split trigonal ground state and excited trigonal state. Macfarlane's g factors for the ground spin-orbit state were in good agreement with spin-resonance results.[7] From the Zeeman structure of the far-infrared spectra, Joyce and Richards[8] obtained reasonable agreement with Macfarlane's calculated g factors for the excited spin-orbit state. The only magnetic measurements reported on this system were by Cottrell *et al.*[9] between 14 and 296 °K. Because of the small temperature dependence, these measurements did not shed much light on the problem.

Reported here are the results of a complete study of the magnetic susceptibility and anisotropy of $Al_2O_3:Ti^{3+}$ over the temperature range 1–350 °K. It is found that the data can be fitted using the previously observed parameters, and estimates of the Van Vleck susceptibility for all three trigonal states are obtained.

II. EXPERIMENT

Since the paramagnetic susceptibilities of interest here are about an order of magnitude smaller than those for $Al_2O_3:V^{3+}$,[10–12] the sensitivity requirements are greater and other experimental problems which arise become more important. These problems must be understood before any reliability can be attached to the final results. Therefore, it will be useful to describe in some detail the apparatus and technique used as well as some of the problems and their solutions.

A. Susceptibility Measurements

The magnetic susceptibilities parallel and perpendicular to the c axis of the crystal were measured at a given temperature by the Faraday method.[13] This is essentially a measurement of the force exerted on a magnetic sample by a nonhomogeneous magnetic field. The force in the direction of the field gradient is given by[14]

$$F_z = m\chi \mathcal{H}_x \frac{\partial \mathcal{H}_x}{\partial z}, \tag{1}$$

where m is the sample mass, χ is the mass susceptibility, and $\mathcal{H}_x \partial \mathcal{H}_x/\partial z$ is the field-gradient product. In general, there could be other terms in the field-gradient product; i.e., $\mathcal{H}_y \partial \mathcal{H}_y/\partial z$ and $\mathcal{H}_z \partial \mathcal{H}_z/\partial z$ as well as forces in other directions. However, by proper location of the sample and a judicious choice of the field geometry, the effect of all of these other terms can be made negligible.

A schematic diagram of the Faraday apparatus is shown in Fig. 1. A Cahn RG-2000 electrobalance with a maximum sensitivity of 0.1 μg was used to measure the magnetic force on the samples when placed in a nonhomogeneous magnetic field. The

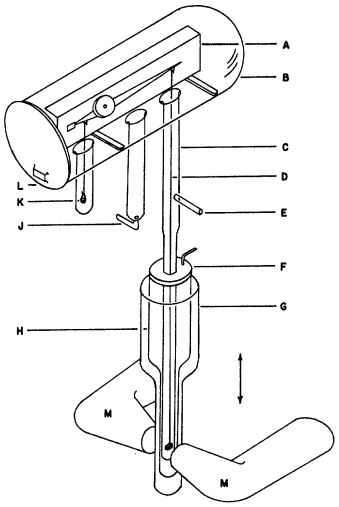

FIG. 1. Diagram of the Faraday balance.

balance weighing mechanism A was enclosed in a glass envelope B which was fitted on one end with a metal end plate L through which electrical connections were made between the balance and its control unit. A Pyrex hangdown tube C was fitted to the envelope by a ground-glass joint, and a fine quartz fiber D was used to suspend the samples from the balance arm. The samples were held in small quartz baskets shaped to fit each one. The hooks between the joints of the quartz fiber were cemented to reduce torsion. Electrical connections into the sample chamber were made through the tube E which was sealed with vacuum wax. The hangdown tube had installed in it a small tubular copper oven with a carbon resistor (26 Ω, 4 W) as a heating element and the sample was suspended inside this tubular oven. The oven was equipped with a Cu-constantan thermocouple and a CryoCal germanium resistance thermometer. The temperature sensors were insulated from their surroundings and mounted within $\frac{1}{4}$ in. of the sample. The thermocouple and Ge thermometer were in thermal contact.

The hangdown tube fits into a double Dewar system used with liquid N_2 in the outer Dewar G and liquid He in the inner Dewar H. The top of the inner Dewar was fitted with a manifold F which was connected to a mechanical vacuum pump. Temperatures to nearly 1 °K could be obtained, under proper conditions, by pumping on the liquid He. A Hg manometer was connected to this system, and the He vapor pressure was used as another indication of the temperature. Tube J was connected to a manifold through which the sample chamber could be evacuated to pressures below 10 μ and refilled to a desired pressure with He gas so that thermal equilibrium between the sample and temperature sensors could be attained.

A 2000-G permanent magnet M with a $2\frac{1}{2}$-in. gap was used to supply the nonhomogeneous field. With the pole pieces used, two regions of equal maximum field-gradient product are symmetrically located on opposite sides of the gap. Measurements made using these two maxima are independent of buoyancy forces, pressure gradients, or other effects dependent on the ambient conditions. The magnet was moved up and down past the sample by means of a motorized hydraulic jack. Data were taken during the descent of the magnet since this speed could be adjusted to allow the balance output to follow the magnet.

As the magnet moved downward, the output of the Cahn balance, which is proportional to the magnetic force, was continuously recorded on a strip-chart recorder, using 10-in. chart paper with 100 divisions. Full scale deflection was 1 mV with zero center. The recorder dead band was a function of the scale factor of the Cahn balance, but in all cases was no more than about $\frac{1}{10}$ division. The emf from both temperature sensors was measured with a Leeds and Northrup K-4 potentiometer.

The force measurements were made by allowing the magnet to pass by the sample, thus producing a maximum magnetic force in one direction, then zero force at the center of the gap where the gradient is zero, then a maximum force in the opposite direction as the gradient changed sign. This was indicated by a sinusoidal curve on the strip-chart recorder similar to the point-by-point curve obtained from the deflection of a quartz helix.[15] The magnetic force is then half the peak-to-peak amplitude of the curve. Some measurements had to be made with smaller signal-to-noise ratio than others. In each case, the noise was of sufficiently high frequency relative to signal frequency that a reasonably good average of the superimposed noise signal could be used as the signal. Under some experimental conditions, a slight drift in apparent sample weight was observed. Data were taken only if the drift was sufficiently linear to allow a quantitative correction to be made for it.

It is obvious from Eq. (1) that in order to obtain the susceptibility from a force measurement, the field-gradient product must be known. It is possible to obtain this from a map of the field, but there are numerous difficulties to this approach. A more direct method is to measure the force on a sample whose susceptibility is accurately known. There are several materials which could be used, e.g., glycerin, distilled water, and copper sulfate. Also χ for Pt and Pd has been measured by several investigators, but the only two values which state the accuracy are for Pt. These are (at 20 °C) (i)

$(0.969 \pm 0.0015) \times 10^{-6}$ emu/g,[15] (ii) $(0.9712 \pm 0.0007) \times 10^{-6}$ emu/g.[16] The value in (i) was the mean of 39 determinations using a quartz helix for the weighing mechanism. The field gradient was obtained by mapping the field with a standardized gaussmeter. The value in (ii) was obtained by the Guoy method. To determine the field-gradient product used in the research reported here, the one value common to (i) and (ii) above, namely, $(0.9705 \pm 0.0015) \times 10^{-6}$ emu/g, was used as a reference value for a temperature-dependence study of the susceptibility for Pt. The field-gradient product was determined from these data and then used in a similar study on Pd. An extremely good fit of the Pd data was obtained, thus giving some confidence in the calibration of the field-gradient product.

There is, however, another problem associated with the calibration which arises when different size samples are used. This is the problem of knowing the volume over which the field-gradient product is uniform. To determine this, six different sized samples of undoped Al_2O_3 were cut from adjacent spaces in a single-crystal boule and were approximately cubical in shape. The smallest of these had a volume very near that of the Pt standard sample used for the calibration. From Eq. (1), F/m at room temperature should be a constant for sample sizes ranging over the volume of uniform field-gradient product. This was found to be the case for a volume up to approximately 200 mm^3 which was larger than any of the actual samples studied. It was found, however, that surface effects, either from the saw or from handling, contributed significantly to the measured F/m and the above result was obtained after repeatedly lapping and cleaning each sample in hot methyl alcohol.

B. Anisotropy Measurements

A magnetically anisotropic sample in a homogeneous magnetic field experiences a torque which is proportional to $\Delta\chi (\equiv \chi_\perp - \chi_\parallel)$, where $\chi_\perp$ and $\chi_\parallel$ are the magnetic susceptibilities perpendicular and parallel to the c axis of the crystal, respectively. To measure $\Delta\chi$, a torsion balance (shown in Fig. 2) was constructed. This balance is essentially identical to that used by Brumage, Quade, and Lin[10] and is the same as that used in our previous work.[11,12]

The principal part of the torsion balance consists of a converted Dolezalek quadrant electrometer E. It is supported by a copper pump plate G and enclosed by a bell jar F. Vacuum connections were made to the pump plate to accommodate a mechanical vacuum pump, an inlet for helium exchange gas, an outlet for attaching a thermocouple vacuum gauge, and an outlet to a mercury manometer. The vacuum gauge is used to measure pressures in the 0–1000-μ range and the mercury manometer is used to measure pressures from 1000 μ to atmospheric. Electrical feed throughs soldered into the pump plate provide a means to pass voltages from the outside to the electrometer. A vacuum connection H of the type normally used to connect ion gauges to vacuum systems was soldered to the under side of the pump plate. This connection provides support and vacuum seal for a hangdown tube C hanging vertically between the pole pieces of the magnet. An opening in the top of the bell jar is fitted with a screw-type adjustment K linked mechanically to an adapter fastened to the manual adjustment knob of the electrometer. This device is vacuum sealed and it provides a means of zeroing the electrometer from the outside.

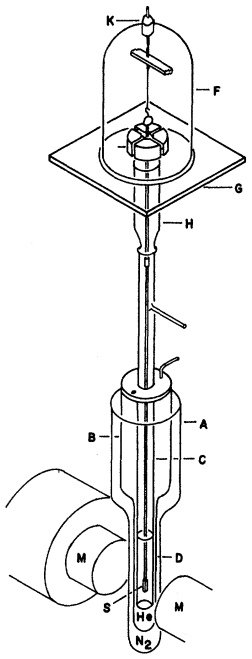

FIG. 2. Diagram of the torsion balance.

A quartz rod was glued to the under side of the electrometer vane. The lower end of this rod, which hangs just below the vacuum connection for the hangdown tube, is connected to a second quartz rod by means of a nonrotating hook assembly. The lower end of the longer rod is fused to a small quartz plate to which the sample S is attached.

The suspended sample hangs inside an oven D at the lower end of the hangdown tube. The oven consists of nichrome wire wound noninductively on a thin-walled cylindrical Teflon form. The sample hangs in the center of the oven a few mm above a Cu-constantan thermocouple junction and resistance

thermometer which are in thermal contact with each other but are insulated from the oven by a rubber holder which fits into the bottom of the oven. The germanium resistance thermometer is used for temperature measurements in the 0–30 °K range and the thermocouple is used in the 30–400 °K range.

The homogeneous magnetic field is produced by a rotatable Varian 4-in. electromagnet M with its regulated power supply and heat exchanger.

The hangdown tube is suspended inside a liquid-He Dewar B and a liquid-N_2 Dewar A. The top of the liquid-helium Dewar is fitted with a copper vacuum jacket. The copper jacket has connections for attaching a mechanical vacuum pump, a thermocouple vacuum gauge, and a manometer to the liquid-helium system, and has an O-ring sealed opening in the top to accommodate a liquid-helium transfer tube.

The installation of an oil-filled damping cup on the balance allowed sequential measurements to be taken much more rapidly and also smoothed out the fluctuations in the balance displacements caused by convection currents in the hangdown tube. A 2-m optical lever, using light reflected off the balance mirror just above the electrometer quadrants, was used for calibrating and aligning the balance as well as observing the balance deflections during the experiment. This distance was long enough to allow very small deflections of the balance to be observed.

The equation for the torque acting on a magnetically anisotropic sample in a homogeneous magnetic field is given by[17]

$$L_M = \tfrac{1}{2} m(\Delta\chi)\mathcal{H}^2 \sin 2\theta\,, \tag{2}$$

where m is the mass of the sample, $\Delta\chi \equiv \chi_\perp - \chi_\parallel$, $\mathcal{H}$ is the field strength, and θ is the angle between the field direction and the c axis of the crystal. Instead of finding this torque from the angle of rotation and the torsion constant of the fiber in order to obtain $\Delta\chi$, the electrometer was used to produce a counter electrical torque given by[18]

$$L_E = -\,cV_q(V_v - \tfrac{1}{2}V_q)\,, \tag{3}$$

where c is a constant depending upon the geometry, V_q is the quadrant voltage, and V_v is the vane voltage. These two torques can be made equal by keeping L_E constant and varying the magnetic field until a null condition is obtained or keeping L_M constant and varying the electrometer voltages or a combination of both. The technique used was similar to that used by Brumage, Quade, and Lin[10] except that with the constant-voltage method the field was monitored by a gaussmeter rather than using the magnet current.

C. Temperature Measurements

For measuring temperatures in the 0–30 °K range, a CryoCal germanium resistance thermometer was used. The physical location of the thermometer was described in Secs. II A and II B. The thermometer was supplied by CryoCal with room-temperature, liquid-nitrogen-dip, and liquid-helium-dip calibration points. The thermometer was further calibrated against a calibrated Cryo resistor manufactured by CryoCal, Inc., over the temperature range 1.72–24.6 °K. For temperature measurements below 1.72 °K and a few degrees above 24.6 °K, an extrapolation of this calibration was used.

An error analysis of the calibrated thermometer, as well as the error in the calibration of the CryoCal standard, and plotting errors, resulted in an error of ±1.0% in the temperatures obtained from measurements by the resistance thermometer. A further check on the accuracy of the temperatures obtained from the resistance thermometer was made by comparing the temperatures obtained from the resistance thermometer against those obtained from measuring the vapor pressure of liquid helium at various points below 4.2 °K and determining the temperature from He^4-vapor-pressure tables obtained from NBS. The agreement was always well within the ±1% error.

The Cu-constantan thermocouples were used for temperature measurements above 30 °K. The thermocouple emf's were measured by the K-4 potentiometer and the temperatures found from calibration tables furnished by Leeds and Northrup. The reference temperature was an ice bath maintained at 0 °C. The thermocouple junction and the resistance thermometer were in thermal contact as described in Secs. II A and II B, and the accuracy of the thermocouples was verified by comparing the measurements of the two sensors at low temperatures.

To make sure that the temperature sensors measured the temperature of the sample, helium exchange gas was used in the sample chambers. To find out what pressure of exchange gas was necessary to ensure thermal equilibrium between the sample and the temperature sensors, the sample was replaced by a germanium resistance thermometer and the helium exchange gas pressure was varied while the two resistance thermometers were simultaneously monitored. The results showed that the two thermometers agree within their error limits (±1.0%) for exchange gas pressures greater than 1 cm Hg, and the agreement is not improved for pressures greater than 10 cm Hg. It should be noted that these results were obtained for time intervals between data points ranging from 1 to 10

min. The agreement is considerably improved if longer time intervals are used. During the experiments, time intervals on the order of 20 min between temperature changes were used when possible.

Lower pressures of exchange gas were sometimes used in the Faraday measurements because of noise problems caused by convection currents, however, longer time intervals between data points were used to allow for thermal equilibrium.

D. Samples

The Al_2O_3 and $Al_2O_3:Ti^{3+}$ single-crystal samples used in this study were made available by Quade who obtained them from the Linde Co. They were oriented by Laue backreflection techniques and the Ti-doped sample was cut to have rectangular sides of approximately $7 \times 5.5 \times 5$ mm. The c axis was perpendicular to a face of the crystal. The samples were polished, boiled in distilled water and in methanol, and weighed. The Ti-doped sample weighed 569.06 mg and had a nominal Ti concentration of 0.1%. This sample contained light and dark striations perpendicular to the c axis, indicating a nonuniform distribution of impurity ions. The darker layers suggested a concentration high enough to have Ti^{3+} pairs, or even clusters, formed, and if this were the case, one could expect a field-dependent susceptibility and anisotropy.

To check the above hypothesis, the sample was installed in the balance, and the anisotropy measured using the combination method mentioned in Sec. IIB above. $\Delta\chi$ was calculated for each voltage and field setting for which a null condition was obtained and then plotted against field. This was done at 298, 4.12, and 1.49 °K. The results are shown in Fig. 3. Also shown in this figure are the results of the same experiment after the sample has been heat treated in air at 1200 °C for 24 h. It can be seen that the field dependence was essentially removed by the heat treatment, except at 1.49 °K, and this will be discussed later in connection with the actual data. This type of heat treatment has recently been shown to break up iron clusters in Fe-doped Al_2O_3,[19] and it appears that the same thing has been accomplished here.

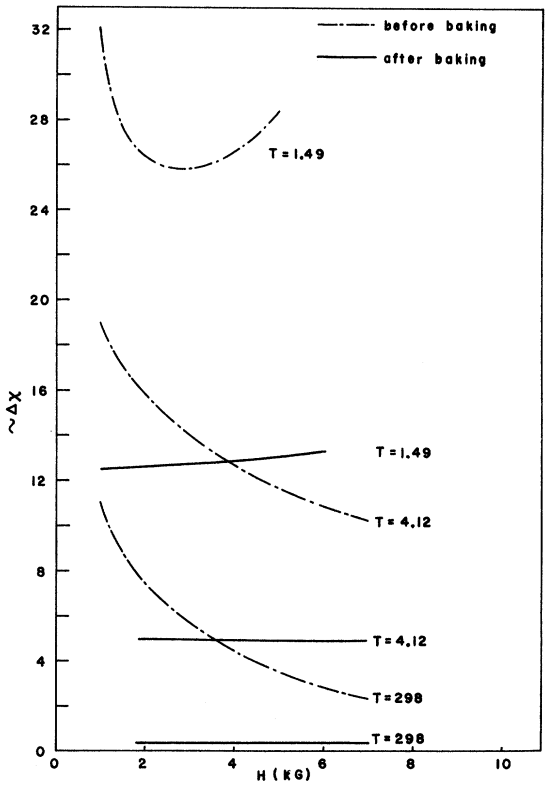

FIG. 3. Effect of heat treating the $Al_2O_3:Ti^{3+}$ sample.

III. MAGNETIC SUSCEPTIBILITY OF Al_2O_3 HOST

The measured susceptibilities are the sum of the diamagnetic and paramagnetic susceptibilities. Since the latter was expected to be very small and was the main interest in this work, it was necessary to know very accurately the diamagnetic susceptibility of the host crystal. This is the case for the Faraday measurements of $\chi_\perp$ and $\chi_\parallel$, however, as long as the diamagnetism is isotropic, it is unimportant for the analysis of the anisotropy data.

The susceptibility of "pure" Al_2O_3 has been reported, to our knowledge, by only five investigators: Herroun and Wilson,[20] Hüttig,[21] Prasad *et al.*,[22] MacClelland and Donoghue,[23] and Fugate and Swenson.[24] The first four of these are cited in the compilation of susceptibilities by Föex.[25] The results of Hüttig are for powdered samples for which the sample density is required to obtain specific mass susceptibility. This undoubtedly is quite different from the density of the single crystal. Furthermore, the results are rendered unreliable because of the scant details in the experimental technique and data analysis. Although Föex cites the work of Prasad *et al.*, no value for "pure" Al_2O_3 was found in it. MacClelland and Donoghue report a value of -0.353×10^{-6} emu/g, which differs from the value of -0.363×10^{-6} emu/g reported by Föex. They do claim an experimental error of 1%, but they give no indication that the result was arrived at by a temperature study. Fugate and Swenson made only an order-of-magnitude measurement using an induction method. Thus, for the purpose of this work, no acceptable value for the diamagnetic susceptibility of single-crystal Al_2O_3 could be found.

The Faraday method, as described in Sec. IIA, was used to measure the susceptibility of the lar-

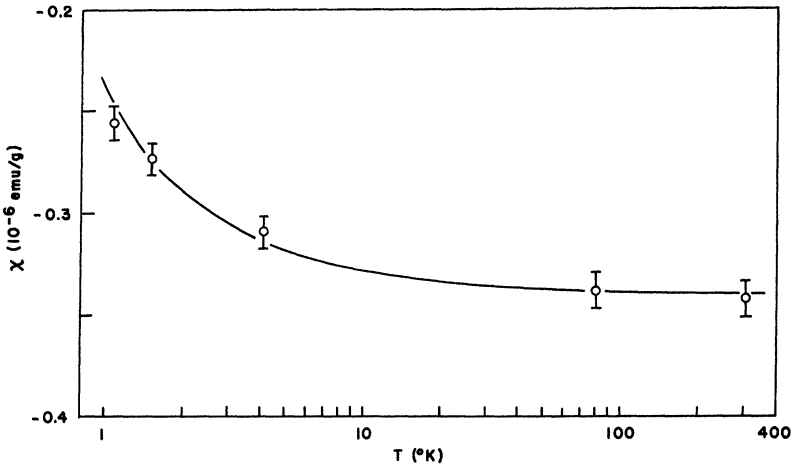

FIG. 4. Diamagnetic susceptibility of "pure" Al_2O_3.

gest of the five samples used to study the uniformity of the field-gradient product. By doing this over the range 1–300 °K, it was also possible to obtain a quantitative estimate of the effect of a few ppm of unwanted impurities. The results are shown in Fig. 4. All the measurements were taken parallel and perpendicular to the crystalline c axis and the results were isotropic within the experimental error. Each datum point is the average of 20 determinations, 10 each in the two directions. Because of this isotropy and the spectroscopic analysis supplied with the sample which indicated the possibility of a few ppm Mn and Fe, the data were fit by least squares to a Curie law of the form

$$\chi = C/T + \chi_{\text{diam}}, \tag{4}$$

where $C = N\mu_0^2 g^2 S(S+1)/3k$. Since Mn^{2+} and Fe^{3+} are both S-state ions they should behave as pure spin systems except for a small S-state splitting which can be ignored in susceptibility studies. Thus, $S = \frac{5}{2}$ and $g = 2.00$.[26,27] These values were used in the least-squares analysis with N the number of impurity ions and χ_{diam} as parameters. The results gave N to correspond to approximately 7 ppm of an S-state impurity and

$$\chi_{\text{diam}} = (-0.339 \pm 0.005) \times 10^{-6} \text{ emu/g}.$$

This is about 6.5% smaller in magnitude than the value of -0.363×10^{-6} emu/g cited by Föex[25] for powder samples and was reproducible when other single-crystal samples were used. Furthermore, it was found to be the only value which would give acceptable fits to the susceptibility data for Al_2O_3: V^{3+} [12] and Al_2O_3:Ti^{3+}.

To check the consistency of the above value, several other single crystals were measured.[28] These were $SrCl_2$, KCl, NaCl, CaF_2, and MgO:Mn^{2+}. Except for $SrCl_2$, only the oxides showed a reasonable deviation from the Föex table.[25] This is believed to be due to the fact that the densities of the cloride and fluoride powders are closer to their crystal densities than is the case with the oxides. Thus, the above value for the diamagnetic susceptibility of single-crystal Al_2O_3 will be used in Sec. IV.

IV. MAGNETIC SUSCEPTIBILITY OF Al_2O_3:Ti^{3+}

A. Theory

The energy-level scheme for a single $3d$ electron in an octahedral field with a small trigonal distortion is shown in Fig. 5, where the three lowest-lying levels are all Kramers doublets. The dynamic Jahn-Teller effect does not alter the splitting scheme but does reduce the level separations. As mentioned earlier, Macfarlane has calculated

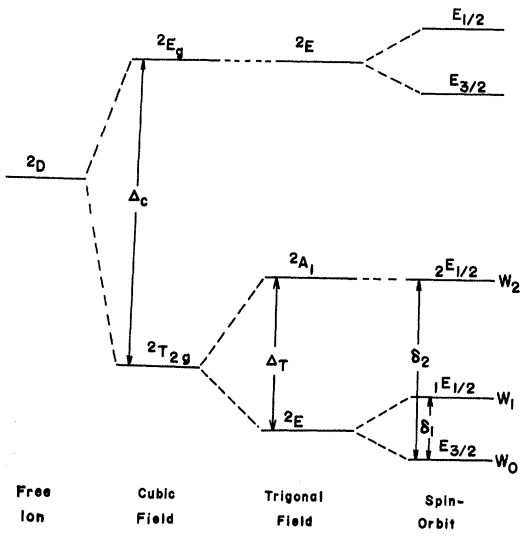

FIG. 5. Energy-level scheme for $(3d)^1$ in Al_2O_3.

the energy-level splittings and g factors, and, in principle, his results could be used to obtain expressions for the susceptibilities. However, such expressions would contain a number of parameters which have not been firmly established, among them being the Jahn-Teller energy and the orbital-reduction factor. Therefore, an analysis similar to the $Al_2O_3:V^{3+}$ system is not possible. Instead a more phenomenological approach is taken, in which only the measured parameters are used.

For a level scheme composed of three Kramers doublets, the paramagnetic susceptibility can be written as[29]

$$\chi_p = N\sum_{i=1}^{3}\left(\frac{W_i'^2}{kT} - 2W_i''\right)e^{-W_i^0/kT}\Big/\sum_{i=1}^{3}e^{-W_i^0/kT}, \quad (5)$$

where the energy for each level has been expanded as

$$W_i = W_i^0 + W_i'\mathcal{H} + W_i''\mathcal{H}^2. \quad (6)$$

Letting $W_i' = \pm\frac{1}{2}g_i\mu_0$ and $\chi_{VVi} = -2NW_i''$, this can be written as

$$\chi_p = B\left[\frac{N\mu_0^2 g_0^2}{4kT} + \chi_{VV0} + \left(\frac{N\mu_0^2 g_1^2}{4kT} + \chi_{VV1}\right)e^{-\delta_1/kT} + \left(\frac{N\mu_0^2 g_2^2}{4kT} + \chi_{VV2}\right)e^{-\delta_2/kT}\right], \quad (7)$$

where

$$B \equiv [1 + \exp(-\delta_1/kT) + \exp(-\delta_2/kT)]^{-1} \quad (8)$$

and

$$\delta_1 \equiv W_1^0 - W_0^0, \quad \delta_2 \equiv W_2^0 - W_0^0.$$

In Eq. (7), g_i is the spectroscopic splitting factor, μ_0 is the Bohr magneton, k is Boltzmann's constant, T is absolute temperature, and N is the concentration of Ti^{3+} ions per g of sample. Equation (7) gives both $\chi_\parallel$ and $\chi_\perp$ by substituting different possible values for the g factors and for χ_{VVi}. The anistropic susceptibility $\Delta\chi(\equiv\chi_\perp - \chi_\parallel)$ is obtained by subtracting the two expressions with the result

TABLE I. Reported parameters for $Al_2O_3:Ti^{3+}$.

Parameter	Value	Type expt	Ref.
$g_{0\parallel}$	1.067	ESR	7
$g_{0\perp}$	<0.1	ESR	7
$g_{1\parallel}$	2.0	IR	8
$g_{1\perp}$	0.0	IR	8
$g_{2\parallel}$	1.9	(Calc)	6
$g_{2\perp}$	2.0	(Calc)	6
δ_1	37.8 cm^{-1}	IR	5,8
δ_2	107.5 cm^{-1}	IR	5,8

$$\Delta\chi = B\{(N\mu_0^2/4kT)[(g_{0\perp}^2 - g_{0\parallel}^2) + (g_{1\perp}^2 - g_{1\parallel}^2)e^{-\delta_1/kT} + (g_{2\perp}^2 - g_{2\parallel}^2)e^{-\delta_2/kT}] + \Delta\chi_{VV0} + \Delta\chi_{VV1}e^{-\delta_1/kT} + \Delta\chi_{VV2}e^{-\delta_2/kT}\}. \quad (9)$$

Those parameters in Eqs. (7) and (9) which have been reported from other measurements, or calculated, are given in Table I. If the parameters of Table I are used in Eqs. (7) and (9), the only unknown parameters left are N and the Van Vleck susceptibilities, however, $g_{2\parallel}$ and $g_{2\perp}$ have not been reported experimentally.

B. Anisotropy Measurements

Anisotropy measurements were made according to the description in Sec. II B on a 569.06-mg sample of $Al_2O_3:Ti^{3+}$ over the temperature range 1.10–342 °K. This sample was the one subjected to the heat treatment as discussed in Sec. II D. The results of the experiment and analysis of the data are shown in Fig. 6. These results as shown depend on the reference value for $\Delta\chi$. This reference was obtained from the Faraday measurements at 4.13 °K and was $\Delta\chi = (-0.0411 \pm 0.005)\times10^{-6}$ emu/g sample. The temperature errors have been incorporated into the total error on $\Delta\chi$ and, in Fig. 6, typical error bars are shown for the various temperature regions. Excluding the data below 3 °K, the analysis was done in the three temperature regions: (a) $T \leq 10$ °K, (b) $T \leq 40$ °K, and (c) $T \leq 350$ °K. In region (a), the contribution to $\Delta\chi$ from the first and second excited states (W_1 and W_2 in Fig. 5) is negligible and only the ground-state susceptibility expression was used. For region (b), the contribution from the second excited state is negligible so it is omitted from the theoretical expression. In region (c), all three states are considered. This three-step analysis is discussed below.

Region (a)

For $T \leq 10$ °K, Eq. (9) reduces to

$$\Delta\chi_0 = -(N\mu_0^2 g_{0\parallel}^2/4kT) + \Delta\chi_{VV0}. \quad (10)$$

In Eq. (10), $g_{0\perp}$ does not appear since it is zero from symmetry arguments.[6] Using $g_{0\parallel} = 1.067$, a least-squares fit was made to the data with the results

$$N = (1.07 \pm 0.15)\times10^{18}\text{-ions/g sample}, \quad \Delta\chi_{VV0} = (6.5 \pm 1.4)\times10^{-9}\text{ emu/g}. \quad (11)$$

Equation (10), using these parameters, gives curve a in Fig. 6.

Region (b)

Using the ground and first excited state, the $\Delta\chi$ expression is

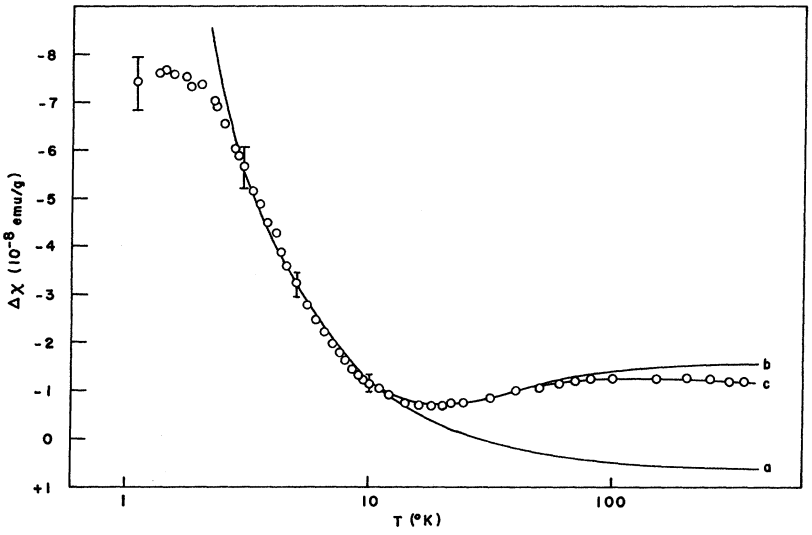

FIG. 6. Magnetic anistropy of $Al_2O_3 : Ti^{3+}$.

$$\Delta\chi_{0,1}=\left(\frac{N\mu_0^2}{4kT}\left(-g_{0\parallel}^2-g_{1\parallel}^2 e^{-\delta_1/kT}\right)+\Delta\chi_{VV0}+\Delta\chi_{VV1}e^{-\delta_1/kT}\right)\Big/\left(1+e^{-\delta_1/kT}\right), \tag{12}$$

where $g_{1\perp}=0.$[6,8] Using the measured values from Table I and the values obtained above for N and $\Delta\chi_{VV0}$ and performing a least-squares fit to the data below 40 °K with $\Delta\chi_{VV1}$ as the adjustable parameter, one obtains

$$\Delta\chi_{VV1}=(-3.8\pm0.8)\times10^{-8}\ \text{emu/g}. \tag{13}$$

Equation (12) with these parameters gives curve b in Fig. 6.

Region (c)

This region actually covers the entire temperature range and Eq. (9) must be used. A two-parameter least-squares fit of this equation to all of the data, using measured values and the results from regions (a) and (b), gives

$$\Delta\chi_{VV2}=(-2.3\pm0.5)\times10^{-9}\ \text{emu/g},\qquad g_{2\perp}^2-g_{2\parallel}^2=-0.40\pm0.05. \tag{14}$$

Equation (9) using all of the above parameters produces curve c in Fig. 6.

The errors for the parameters in region (a) were determined from standard least-squares formulas, while the errors for the parameters in regions (b) and (c) were obtained by incorporating into the data the errors in the experiment, and performing least-squares analyses on the corrected data to find how the parameters changed due to error corrections. All of the parameters determined from this analysis are then

$$\begin{aligned}N&=(1.07\pm0.15)\times10^{18}\text{-ions/g sample},\\ \Delta\chi_{VV0}&=(6.5\pm1.4)\times10^{-9}\ \text{emu/g},\\ \Delta\chi_{VV1}&=(-3.8\pm0.8)\times10^{-8}\ \text{emu/g},\\ \Delta\chi_{VV2}&=(-2.3\pm0.5)\times10^{-9}\ \text{emu/g},\\ g_{2\perp}^2-g_{2\parallel}^2&=-0.40\pm0.05.\end{aligned} \tag{15}$$

C. Faraday Measurements

Faraday measurements of $\chi_\perp$ and $\chi_\parallel$ were made as described in Sec. IIA between 1 and 300 °K. In this case, the measured susceptibility includes contributions from the diamagnetic host and from an unwanted S-state impurity. The measured susceptibility then has the form

$$\chi_{\parallel,\perp}=\chi_{p\parallel,\perp}+\chi_{diam}+C/T, \tag{16}$$

where $\chi_{diam}=-(0.339\pm0.005)\times10^{-6}$ emu/g from Sec. III and C is the Curie constant associated with the S-state impurity and must be treated as an adjustable parameter.

The experimental and theoretical results are shown in Figs. 7 and 8. The major contribution to the errors is the uncertainty in the field-gradient product. Since this is a systematic error introduced by calculating χ from force measurements, its contribution was easy to incorporate into the total error. Below 12 °K, the random error due to scatter of the data could be calculated and it was added to the systematic error. A random-error analysis for the two excited states was difficult to perform because the Boltzmann factor makes contributions from these upper levels rather small. If it is assumed to be as large as the random error for the ground-state data, then the total uncertainty in the parameters associated with these two levels

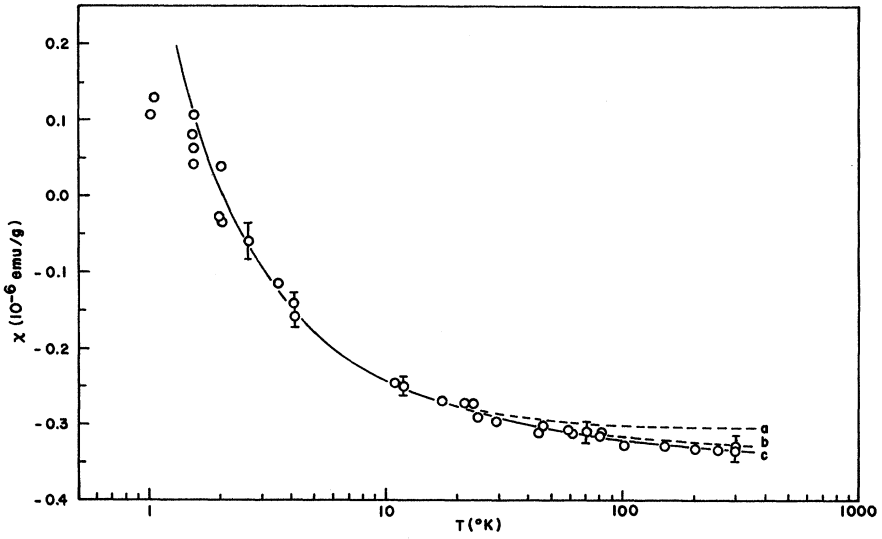

FIG. 7. Measured susceptibility of $Al_2O_3:Ti^{3+}$, H perpendicular to c axis.

is of the order of 100%. This implies that the results only represent an order of magnitude, but it is found that the parameters determined here are in reasonably good agreement with those from the $\Delta\chi$ experiment. In addition, the C/T term in Eq. (16) contributes to the total error.

The data analysis was carried out in the same three temperature regions as was the $\Delta\chi$ analysis, and, where applicable, the parameters of Table I were used.

Region (a)

As before, only the ground state contributes to χ_p and Eq. (16) becomes

$$\chi_\perp = \chi_{VV0\perp} + \chi_{diam} + C/T, \tag{17}$$

$$\chi_\parallel = (N\mu_0^2 g_{0\parallel}^2/4kT) + \chi_{VV0\parallel} + \chi_{diam} + C/T. \tag{18}$$

Equation (17) was used in a least-squares program to determine $\chi_{VV0\perp}$ and C. Equation (18) was then used to obtain $\chi_{VV0\parallel}$ and N with the results

$$\begin{aligned} \chi_{VV0\perp} &= (0.031 \pm 0.019) \times 10^{-6} \text{ emu/g}, \\ \chi_{VV0\parallel} &= (0.024 \pm 0.018) \times 10^{-6} \text{ emu/g}, \\ C &= (0.641 \pm 0.037) \times 10^{-6} \text{ emu °K/g}, \\ N &= (1.06 \pm 0.21) \times 10^{18} \ Ti^{3+} \text{ ions/g sample}. \end{aligned} \tag{19}$$

Using these parameters, Eqs. (17) and (18) give curve a in Figs. 7 and 8.

Region (b)

The ground and first excited state are involved here and Eq. (16) becomes

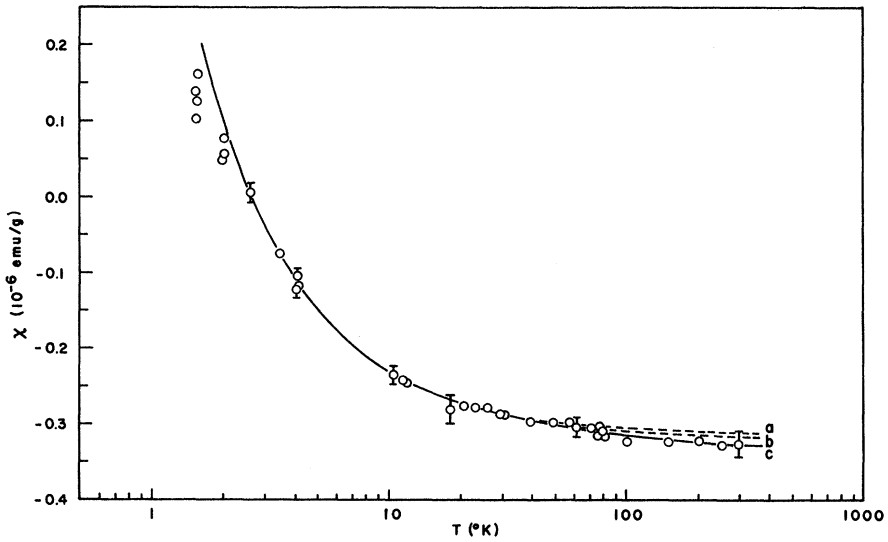

FIG. 8. Measured susceptibility of $Al_2O_3:Ti^{3+}$, H parallel to c axis.

$$\chi_\perp = (\chi_{VV0\perp} + \chi_{VV1\perp} e^{-\delta_1/kT})(1 + e^{-\delta_1/kT})^{-1}, \quad (20)$$

$$\chi_\parallel = \left[\frac{N\mu_0^2 g_{0\parallel}^2}{4kT} + \chi_{VV0\parallel} + \left(\frac{N\mu_0^2 g_{1\parallel}^2}{4kT} + \chi_{VV1\parallel}\right) e^{-\delta_1/kT}\right] \times (1 + e^{-\delta_1/kT})^{-1} + \chi_{diam} + C/T. \quad (21)$$

Again, a least-squares program with $\chi_{VV1\parallel,\perp}$ as the parameters gave

$$\chi_{VV1\perp} = -(0.015 \pm 0.015) \times 10^{-6} \text{ emu/g}, \quad \chi_{VV1\parallel} = -(0.013 \pm 0.013) \times 10^{-6} \text{ emu/g}. \quad (22)$$

These theoretical results are shown as curve b in Figs. 7 and 8.

Region (c)

For this temperature range, Eq. (7) must be used in Eq. (16) with the only undetermined parameters being $\chi_{VV2\perp}$ and $\chi_{VV2\parallel}$. Of course, the g factors for the second excited state should be included as adjustable parameters, but it was found that the least-squares fit was essentially independent of these, indicating that

$$|\chi_{VV2}| > N\mu_0^2 g_2^2/4kT.$$

This rather insensitive region gave

$$\chi_{VV2\perp} = -(0.025 \pm 0.020) \times 10^{-6} \text{ emu/g}, \quad \chi_{VV2\parallel} = -(0.025 \pm 0.020) \times 10^{-6} \text{ emu/g}. \quad (23)$$

These results are shown as curve c in Figs. 7 and 8.

V. DISCUSSION

Although the parameters obtained from the Faraday data have large uncertainties, their differences are in reasonable agreement with those obtained from the anisotropy analysis.

In Fig. 6, there are two important features to be noted about these curves. First, the two regional curves fit the data for their respective regions very well, but deviate considerably from the data above their regions. Therefore, the least-squares fits were very sensitive to parameter changes in each region. If the required curve corrections had been small in each region, the parameters for that region would have had very small effects on the curve, leading either to complete indeterminacy in the parameters or large errors in the results.

Second, the curve does not fit the data below about 3 °K. In fact, the data behave in such a way that the theory, which predicts $1/T$ dependence in this region, cannot possibly explain it. The anomaly could not be explained by Brillouin saturation; therefore, there must be some mechanism besides the single-ion susceptibility giving rise to anisotropy in this temperature range.

The simplest explanation would be the presence of exchange effects between magnetic ions, leading to a spontaneous magnetization below an apparent Néel temperature of about 3 °K. The model must have the added feature of giving an anisotropic contribution below the Néel temperature and an isotropic contribution above this point. There are two possibilities: (i) Since the Faraday susceptibilities indicated a relatively high concentration of an assumed S-state impurity (about 25 ppm of sample weight), this low-temperature anisotropy could be due to anisotropic superexchange interactions between these impurity ions, or (ii) some pairs or even clusters of Ti^{3+} ions remain after the heat treatment and form sublattices in local regions throughout the crystal. These "local" sublattices carry a spontaneous magnetization which can be treated by the Néel–Van Vleck theory.[30] The first possibility was investigated by applying Moriya's[31] theory of anisotropic superexchange to Fe^{3+} impurities but the resulting fit of the data was unacceptable even with two adjustable parameters. The second possibility was then explored with the Néel–Van Vleck theory which predicts an anisotropic susceptibility below the Néel temperature which becomes isotropic above this temperature. The expressions for the susceptibilities below the Néel point are

$$\chi_\perp = C/(T_N - \theta), \quad (24)$$

$$\chi_\parallel = \frac{C \times 3S(S+1)^{-1} B_S'(\epsilon/T)}{T - 3S(S+1)^{-1}\theta B_S'(\epsilon/T)},$$

where B_S is the Brillouin function and B_S' is its derivative, C is the Curie constant, and θ is the Curie temperature. Also,

$$\epsilon = g\mu_0 SnC^{-1} T_N M_j^0/k, \quad (25)$$

where n is the number of sublattices, T_N is the Néel temperature, and M_j^0 is the spontaneous magnetization of the jth sublattice. The expression for $\Delta\chi$ is

$$\Delta\chi_C = \frac{C}{T_N - \theta} - \frac{C[1 - \tanh^2(\epsilon/T)]}{T - \theta[1 - \tanh^2(\epsilon/T)]}, \quad (26)$$

assuming that the interacting ions are Ti^{3+} with $S = \frac{1}{2}$. Adding this coupling term to the susceptibility expression for single Ti^{3+} ions and fitting to the data for $T \leq 3$ °K gives

$$C = 1.80 \times 10^{-10} \text{ cgs emu °K}, \quad T_N = 3.21 \text{ °K}, \quad \theta = 1.53 \text{ °K}, \quad \epsilon = 0.79 \text{ °K}. \quad (27)$$

The value of $N = 1.07 \times 10^{18}$ for the single ions was retained in this analysis. Actually, N and the parameter C of Eq. (26) are interrelated, i.e., N should decrease, while C increases as the temperature is lowered. This complicated temperature

dependence is neglected in the analysis because it is impossible to determine the numbers of single and coupled ions for a given temperature. However, the above value of C corresponds to only 0.03% of the available Ti^{3+} ions.

The results of this analysis are shown as the solid line in Fig. 9. This theory fits the data quite well, but one cannot infer much physical significance from this since four parameters were used in the analysis. However, its advantages over the Moriya theory were clear and do suggest, especially in light of other evidence, that the behavior of the anisotropy below 3 or 4 °K can most likely be attributed to interacting Ti^{3+} ions.

Also plotted in Fig. 9 is the Van Vleck susceptibility for $Al_2O_3:Ti^{3+}$ given by

$$\Delta\chi_{VV} = B(\Delta\chi_{VV0} + \Delta\chi_{VV1} e^{-\delta_1/kT} + \Delta\chi_{VV2} e^{-\delta_2/kT}). \tag{28}$$

One can see that the Van Vleck terms cannot be ignored in this analysis as they were in $Al_2O_3:V^{3+}$, and that the high-temperature $\Delta\chi$ measurements have nearly reached the temperature-independent limit.

From Eq. (15), $g_{2\perp}^2 - g_{2\parallel}^2 = -40 \pm 0.05$, whereas Macfarlane[6] obtains a value of $+0.39$ from his theoretical calculation. In this work, the value for this parameter was allowed to vary over a wide range with the result that any positive value would not reproduce the data within the experimental error. This discrepancy between theory and experiment is still regarded as an open question.

VI. CONCLUSION

$Al_2O_3:Ti^{3+}$ does not lend itself to a magnetic susceptibility study as readily as some of the other transition-metal ions doped into this host, but the experiments, especially the anisotropy measurements, do appear to provide some confirmation of the previously determined parameters listed in Table I. These experiments have also provided reasonable estimates of the Van Vleck susceptibilities for each level and for $g_{2\perp}^2 - g_{2\parallel}^2$ for the second excited state.

An attempt to fit the data with crystal field theory without any Jahn-Teller effect was made. It was found that reasonably good agreement could be obtained for some of the observed quantities if one used slightly different crystal field parameters from those used by Macfarlane. However, this approach always resulted in a value for the orbital reduction factor k which was somewhere between 0.58 and 0.64. This value for k produces an orbital reduction which is too large to assume that covalency is the dominant mechanism for suppressing the energy spacings and reducing $g_{0\parallel}$, but it does suggest that covalency may be significant even with Jahn-Teller coupling. The question of covalency versus Jahn-Teller effect still seems to be unanswered and will remain so until a more explicit determination of the Jahn-Teller energy can be made or until some kind of molecular orbital calculation is made to estimate k from more fundamental principles.

ACKNOWLEDGMENTS

The authors wish to express their appreciation to Professor C. R. Quade for suggesting this problem and supplying the doped and undoped Al_2O_3 crystals. Professor Quade also contributed many helpful discussions during the course of the work. Gratitude is also expressed to Dr. L. A. Boatner and Dr. R. W. Reynolds for supplying some of the

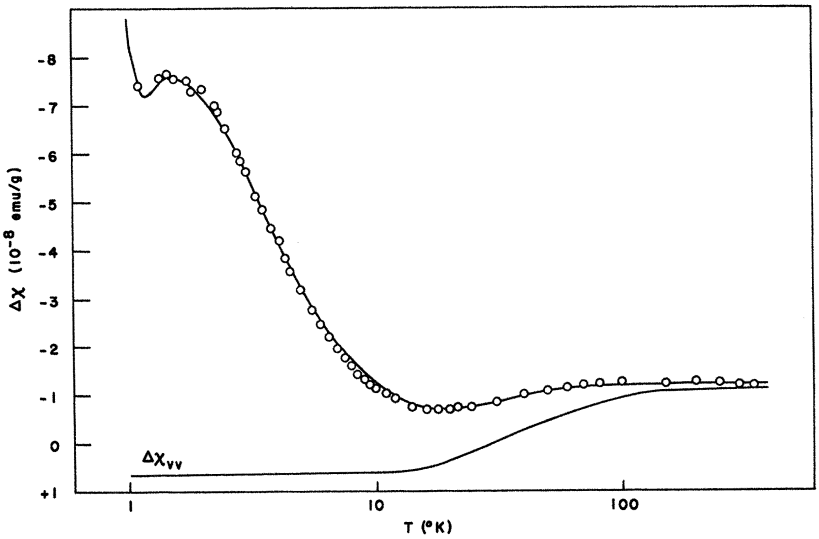

FIG. 9. Magnetic anistropy of $Al_2O_3:Ti^{3+}$ including the Néel–Van Vleck coupling term between Ti^{3+} ions.

host crystals which it became necessary to study and for making some preliminary ESR measurements on some of the samples. The technical assistance of Morris Greenwood is also appreciated.

---

†Work supported by the Advanced Research Projects Agency under Grant No. DAHC 15-70-G1.

[1]H. A. Jahn and E. Teller, Proc. Roy. Soc. (London) A161, 220 (1937).

[2]H. A. Jahn, Proc. Roy. Soc. (London) A164, 117 (1938).

[3]F. S. Ham, Phys. Rev. 138, A1727 (1965).

[4]D. S. McClure, J. Chem. Phys. 36, 2757 (1962).

[5]E. D. Nelson, J. Y. Wong, and A. L. Schawlow, Phys. Rev. 156, 298 (1967).

[6]R. M. Macfarlane, J. Y. Wong, and M. D. Sturge, Phys. Rev. 166, 250 (1968).

[7]N. E. Kask, L. S. Korneinko, T. S. Mandel'shtam, and A. M. Prokhorov, Fiz. Tverd. Tela 5, 2306 (1963) [Soviet Phys. Solid State 5, 1677 (1964)].

[8]R. R. Joyce and P. L. Richards, Phys. Rev. 179, 375 (1969).

[9]T. H. E. Cottrell, N. C. Andreadakis, and C. R. Quade, Phys. Letters 21, 7 (1966).

[10]W. H. Brumage, C. R. Quade, and C. C. Lin, Phys. Rev. 131, 949 (1963).

[11]A. R. Smith and R. W. Mires, Phys. Rev. 172, 265 (1968).

[12]D. J. Arnold, A. R. Smith, and R. W. Mires, Phys. Rev. B 1, 2355 (1970).

[13]L. N. Mulay, *Magnetic Susceptibility* (Interscience, New York, 1963), p. 1829.

[14]L. F. Bates, *Modern Magnetism* (Cambridge U. P., London, 1961), p. 111.

[15]F. E. Senftle, M. D. Lee, A. A. Monkewicz, J. W. Mayo, and T. Pankey, Rev. Sci. Instr. 29, 429 (1958).

[16]F. E. Hoare and J. C. Walling, Proc. Phys. Soc. (London) 64B, 337 (1951).

[17]J. F. Nye, *The Physical Properties of Crystals* (Oxford U. P., New York, 1957), p. 60.

[18]S. G. Starling, *Electricity and Magnetism* (Longmans Green and Company, New York, 1925), pp. 157–161.

[19]V. G. Bhide and S. K. Date, Phys. Rev. 172, 345 (1968).

[20]E. F. Herroun and E. Wilson, Proc. Phys. Soc. (London) 33, 196 (1921).

[21]G. F. Hüttig, Z. Anorg. Allgem. Chem. 224, 225 (1935).

[22]M. Prasad, S. S. Dharmatti, and S. V. Gokhale, Proc. Indian Acad. Sci. A20, 224 (1944).

[23]J. D. MacClelland and J. J. Donoghue, J. Appl. Phys. 24, 963 (1953).

[24]R. Q. Fugate and C. A. Swenson, J. Appl. Phys. 40, 3034 (1969).

[25]G. Föex, *Constantes Selectionees Diamagnetisme et Paramagnetisme Relaxation Paramagnetique* (Masson, Paris, 1957), Vol. 7.

[26]W. Low and J. T. Suss, Phys. Rev. 119, 132 (1960).

[27]G. S. Bogle and H. F. Symmons, Proc. Phys. Soc. (London) 73, 531 (1959).

[28]D. J. Arnold and R. W. Mires, Texas J. Sci. 22, No. 3 (1970).

[29]J. H. Van Vleck, *Electric and Magnetic Susceptibilities* (Oxford U. P., London, 1932), p. 182.

[30]J. H. Van Vleck, J. Chem. Phys. 9, 85 (1941).

[31]T. Moriya, Phys. Rev. 120, 91 (1960).